

# Effect of Fluorination of 2,1,3-Benzothiadiazole

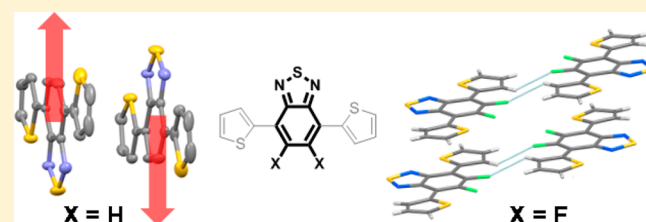
Christian B. Nielsen,<sup>\*,†</sup> Andrew J. P. White,<sup>†</sup> and Iain McCulloch<sup>†,‡</sup>

<sup>†</sup>Department of Chemistry and Centre for Plastic Electronics, Imperial College London, London SW7 2AZ, United Kingdom

<sup>‡</sup>Physical Sciences and Engineering Division, King Abdullah University of Science and Technology (KAUST), Thuwal 23955-6900, Saudi Arabia

## S Supporting Information

**ABSTRACT:** The 4,7-dithieno-2,1,3-benzothiadiazole (DTBT) moiety and its fluorinated counterpart are important  $\pi$ -conjugated building blocks in the field of organic electronics. Here we present a combined experimental and theoretical investigation into fundamental properties relating to these two molecular entities and discuss the potential impact on extended  $\pi$ -conjugated materials and their electronic properties. While the fluorinated derivative, in the solid state, packs with a cofacial overlap smaller than that of DTBT, we report experimental evidence of stronger optical absorption as well as stronger intra- and intermolecular contacts upon fluorination.



experimental evidence of stronger optical absorption as well as stronger intra- and intermolecular contacts upon fluorination.

## INTRODUCTION

The highly electron-deficient 2,1,3-benzothiadiazole unit is one of the most popular building blocks in organic electronics. Especially when designing molecularly hybridized push-pull type materials, where the alternating arrangement of electron-rich and electron-deficient units along the  $\pi$ -conjugated backbone effectively controls the frontier molecular orbitals, 2,1,3-benzothiadiazole is often the electron-deficient unit of choice.<sup>1–4</sup> To further fine-tune the frontier molecular orbitals as well as other important materials parameters such as solubility and crystallinity, chemical modifications of the 2,1,3-benzothiadiazole unit have attracted much interest.<sup>5–8</sup> In particular, fluorination has been shown to be an effective way to lower the highest occupied molecular orbital (HOMO) and thus obtain a better performing material for organic photovoltaics because of an improved open-circuit voltage.<sup>9–11</sup>

While the effect of fluorination on the frontier energy levels is well-understood,<sup>9,11</sup> experimental details about the underlying reasons for observed differences relating to solubility, crystallinity, charge carrier mobility, and bulk heterojunction blend morphologies with fullerene acceptors are lacking. Here, we compare the two well-known chromophores 4,7-dithieno-2,1,3-benzothiadiazole (DTBT) and its fluorinated derivative, 5,6-difluoro-4,7-dithieno-2,1,3-benzothiadiazole (DTF2BT), depicted in Figure 1. A detailed study of these two simple model compounds, which are frequently occurring building blocks in numerous high-performing organic electronic materials, highlights some important changes in physical properties upon fluorination.

## RESULTS AND DISCUSSION

DTBT and DTF2BT were synthesized according to literature procedures, and single crystals were obtained from slow evaporation of hexane and toluene solutions, respectively. As

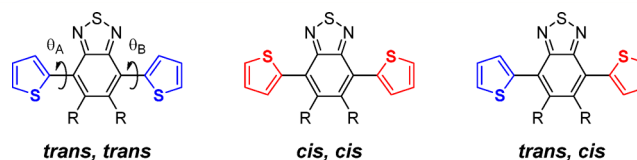


**Figure 1.** Molecular structures of DTBT ( $R = H$ ) and DTF2BT ( $R = F$ ) with different coplanar geometries defined by dihedral (torsional) angles  $\theta_A$  and  $\theta_B$ .

shown in Figure 1, three coplanar conformations exist for the two chromophores. In the obtained crystals, both DTBT and DTF2BT show a strong preference for the trans-cis conformer as illustrated in Figure 2.

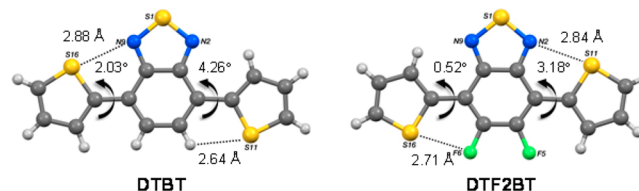


**Figure 2.** Crystal structures of DTBT and DTF2BT with major occupancy orientations displayed (see the Supporting Information for the minor occupancy orientations).

Both crystal structures are disordered though. In the DTBT crystal, approximately 71% of the molecules are in the trans-cis conformation, while the remaining molecules adopt the cis-cis conformation. The DTF2BT crystal, meanwhile, shows minor occupancies of both the trans-trans (~10%) and cis-cis (~27%) conformations. For trans-cis DTBT, dihedral angles

Received: February 24, 2015

Published: April 22, 2015

$\theta_A$  and  $\theta_B$  are  $2.03^\circ$  and  $4.26^\circ$ , respectively, while a slightly higher degree of coplanarity is observed for trans–cis DTF2BT with dihedral angles of  $0.52^\circ$  and  $3.18^\circ$ , respectively, as illustrated in Figure 2. The increased coplanarity of DTF2BT is reflected in short intramolecular contacts; in particular, the S–F and S–N distances ( $2.71$  and  $2.84$  Å, respectively) are significantly shorter than the sum of the van der Waals radii. For comparison, the S–H and S–N intramolecular distances are  $2.64$  and  $2.88$  Å, respectively, in DTBT. Although the thiophenes are obviously disordered in both crystals, the stronger relative representation of the trans conformation in the DTF2BT crystal as well as the higher degree of coplanarity and the short intramolecular S–F contacts are all indications of a planarizing effect from the fluorination of benzothiadiazole.

In contrast to the single-crystal structures, quantum mechanical calculations using Gaussian at the B3LYP/6-31G\* level of theory predict the trans–trans conformation to be most stable for both DTBT and DTF2BT, with the trans–cis conformer being destabilized by  $2.8$  and  $2.0$  kJ mol<sup>-1</sup>, respectively (Table S1 of the Supporting Information). While the torsional degree of freedom has previously been studied theoretically for the two model compounds,<sup>11</sup> we used variable-temperature <sup>1</sup>H NMR to investigate this aspect experimentally. Although the spectral line broadening upon cooling (Figure 3)

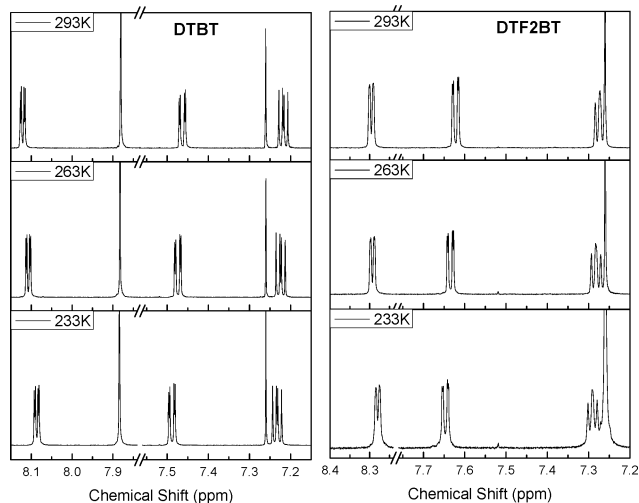


**Figure 3.** Aromatic region of <sup>1</sup>H NMR spectra of DTBT (left) and DTF2BT (right) recorded in CDCl<sub>3</sub> at 293, 263, and 233 K.

appears to be slightly more pronounced for DTF2BT than for DTBT, we were not able to reach the coalescence point in deuterated chloroform at 213 K or in deuterated tetrahydrofuran at 183 K, where  $kT$  is on the order of  $1.5$  kJ mol<sup>-1</sup> (Figures S1–S3 of the Supporting Information). This indicates that the activation barrier for rotation ( $\theta_A$  and  $\theta_B$ ) in solution is significantly smaller than what is predicted theoretically in vacuum.<sup>11,12</sup>

UV–vis spectroscopy was used to investigate the optical properties of DTBT and DTF2BT in solution as illustrated in Figure 4 and summarized in Table 1. Both model compounds show two absorption bands around 300 and 400–450 nm. While the high-energy absorption band coincides for the two compounds and is unaffected by changes in solvent polarity, the low-energy absorption feature is red-shifted approximately 20 nm for DTBT compared to that for DTF2BT. Moreover, DTF2BT shows a stronger solvatochromic effect with a 10 nm

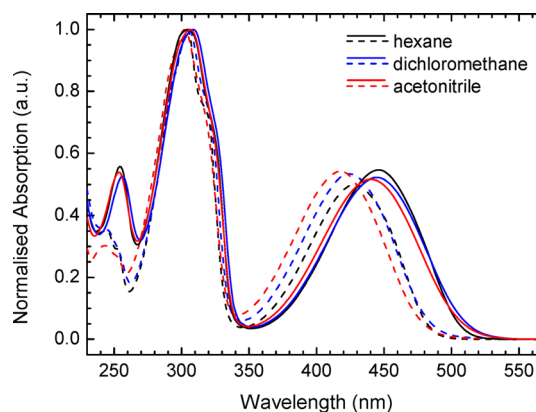


**Figure 4.** Normalized UV–vis spectra of DTBT (solid lines) and DTF2BT (dashed lines) in hexane (black), dichloromethane (blue), and acetonitrile (red) solutions.

blue-shift when going from *n*-hexane to acetonitrile. We also note that the molar extinction coefficient [at both absorption features (Table 1)] is consistently higher for DTF2BT than for DTBT, which of course is of paramount importance when considering these materials for organic photovoltaic applications.<sup>8</sup>

Quantum mechanical calculations were again used to support the experimental details, and as depicted in Table 1, there is a fairly good agreement between the experimental and theoretical optical properties. The optical transition around 300 nm is predominantly from the HOMO to LUMO+1 transition and has  $\pi$ – $\pi^*$  character, while the lower-energy feature is dominated by the HOMO to LUMO transition with strong intramolecular charge transfer (ICT) character. This also explains why the solvatochromism is observed for only the low-energy absorption band.

Turning our attention to the crystal packing of DTBT and DTF2BT (Figure 5 and Table 2), we note that DTBT is an orthorhombic crystal, while DTF2BT is distorted to a monoclinic crystal system with a  $\beta$  angle of  $104.82^\circ$ . Viewing the two crystals along their *a*-axes reveals that both pack in a herringbone type arrangement as often seen for small  $\pi$ -conjugated molecules.<sup>13</sup> As illustrated in Figure 5C, the interplanar distances ( $d_2$ ) between adjacent molecules are nearly identical for the two structures with values of  $3.41$ – $3.44$  Å for DTBT and  $3.44$ – $3.46$  Å for DTF2BT. The slipping distances ( $d_1$ ) are slightly larger for DTF2BT ( $0.94$ – $0.95$  Å) than for DTBT ( $0.75$ – $0.79$  Å), which could potentially affect the charge transport in DTF2BT-based materials adversely.<sup>14,15</sup>

Calculated permanent dipole moments for the three different coplanar conformations for both molecules are depicted in Figure 6. The major occupancy trans–cis conformations have dipole moments of  $1.18$  D (DTBT) and  $0.70$  D (DTF2BT). Importantly, for DTBT, the dipole moment is directed away from the electron-deficient thiadiazole ring, while the dipole moment of DTF2BT, because of its highly electron-withdrawing fluorine substituents, is directed toward the thiadiazole ring as illustrated in Figure 6. For DTBT, the other conformation present in the crystal (cis–cis) has an even stronger dipole moment of  $2.21$  D in the same direction, while the two minor conformations of DTF2BT have oppositely directed dipole moments.<sup>16</sup>

We believe that the large dipole moment of DTBT and the resulting strong dipole–dipole interactions are responsible for the antiparallel alignment of adjacent DTBT molecules

Table 1. Experimental and Theoretical Optical Properties of DTBT and DTF2BT in Solution

	solvent	$\lambda_{\max}$ (nm), experimental	$\epsilon$ ( $\times 10^3$ M $^{-1}$ cm $^{-1}$ ), experimental	$\lambda_{\max}$ (nm), theoretical <sup>a</sup>	oscillator strength, theoretical <sup>a</sup>
DTBT	<i>n</i> -hexane	306, 446	28.5, 15.5	325, 531	0.663, 0.364
	dichloromethane	309, 445	28.9, 15.2	325, 531	0.638, 0.371
	acetonitrile	306, 441	28.8, 14.9	325, 529	0.639, 0.357
DTF2BT	<i>n</i> -hexane	304, 428	33.4, 16.7	323, 518	0.771, 0.367
	dichloromethane	306, 424	31.0, 16.5	323, 513	0.753, 0.386
	acetonitrile	302, 418	29.2, 15.8	322, 510	0.741, 0.375

<sup>a</sup>Determined using Gaussian at the B3LYP/6-31G\* level of theory.

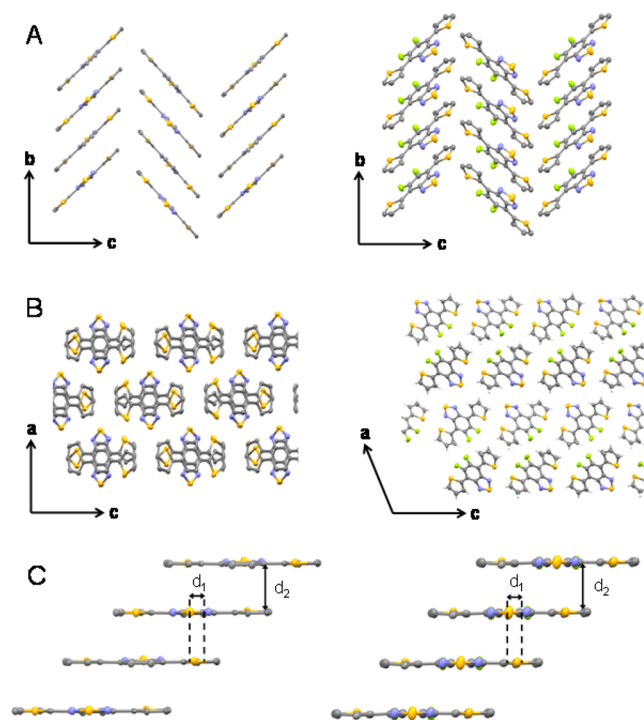


Figure 5. Crystal packing of DTBT (left) and DTF2BT (right) viewed along the *a*-axis (A) and *b*-axis (B) and showing the slipping distance ( $d_1$ ) and the interplanar distance ( $d_2$ ) (C).

Table 2. Crystal Systems, Space Groups, and Lattice Parameters for DTBT and DTF2BT Crystals

	DTBT	DTF2BT
crystal system	orthorhombic	monoclinic
space group	<i>Pbca</i>	<i>P2<sub>1</sub>/c</i>
<i>a</i> , <i>b</i> , <i>c</i> (Å)	12.73, 9.88, 20.05	15.73, 4.81, 17.75
$\alpha$ , $\beta$ , $\gamma$ (deg)	90, 90, 90	90, 104.82, 90

depicted in Figure 6B. DTF2BT, on the other hand, has a much smaller permanent dipole moment, and adjacent molecules are consequently observed to align in a parallel fashion along the  $\pi$ -stacking direction (Figure 6B). The change in direction of the dipole moment for DTF2BT with different conformations could potentially account for some stabilizing dipole–dipole interactions in the crystal, but we find it unlikely to be the major driving force for this parallel packing. Instead, we note that adjacent  $\pi$ -stacks of DTF2BT have particularly close H–F contacts (2.51 Å) as illustrated in Figure 6C. Each DTF2BT molecule partakes in two intermolecular H–F interactions, while no similar intermolecular interactions could be observed for DTBT. Although we believe that these observations are the major factors governing the molecular packing motifs of DTBT

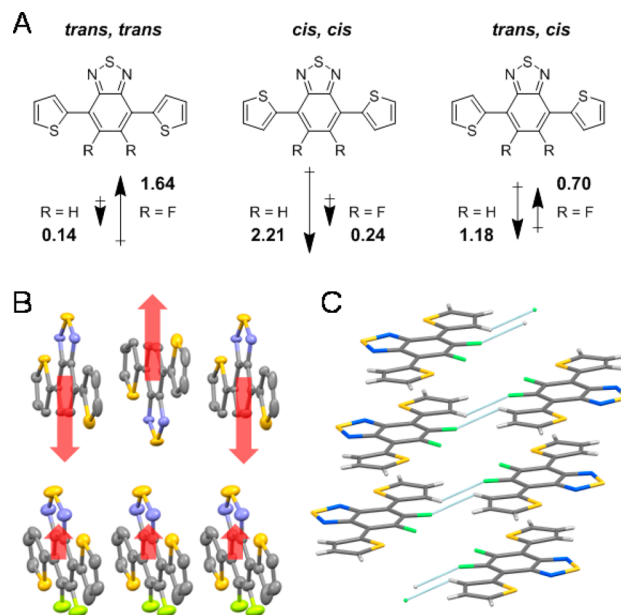
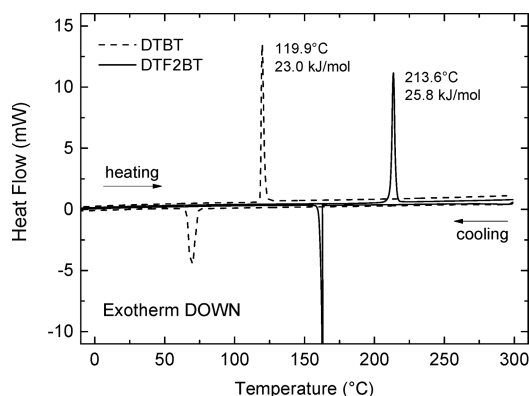


Figure 6. Calculated dipole moments for the three coplanar conformations of DTBT and DTF2BT (A), the alignment of dipole moments in the  $\pi$ -stacking direction (B), and intermolecular H–F interactions in the DTF2BT crystal (C).

and DTF2BT, it is worth noting that there are other potential intermolecular interactions that could affect the molecular packing.<sup>17</sup>

Taking into account the different conformations and their different permanent dipole moments, we think it is worth noting that the polarity of the solvent used during solution processing of DTBT- and DTF2BT-containing materials is likely to affect the distribution of conformations and thus also the solid state packing.<sup>16</sup> In that context, it is also worth noting that the two crystal structures are obtained from solvents with slightly different polarities.

The thermal properties of DTBT and DTF2BT were investigated with differential scanning calorimetry (DSC). In both cases, only one phase transition from solid to isotropic melt was observed in the temperature range of 0–300 °C as illustrated in Figure 7. DTBT has a melting point of 119.9 °C with an enthalpy of melting of 23.0 kJ/mol, while DTF2BT melts at 213.6 °C with an enthalpy of melting of 25.8 kJ/mol. As the two chromophores have similar molecular symmetries and comparable conformational disorders in terms of cis/trans isomerism, the much higher melting point of DTF2BT compared to that of DTBT is most likely to stem from stronger intermolecular forces in the case of DTF2BT. This is in good agreement with the sharper crystallization peak for DTF2BT upon cooling as well as the crystal packing discussed above. Although DTBT shows intermolecular dipole–dipole



**Figure 7.** DSC traces of DTBT (---) and DTF2BT (—) recorded at  $10\text{ }^{\circ}\text{C min}^{-1}$  under nitrogen.

interactions, these are likely weak because of the slip-stacked nature of the packing with each 2,1,3-benzothiadiazole unit interacting with neighboring thiophene units rather than neighboring 2,1,3-benzothiadiazole units, which is evident from Figure 5C. DTF2BT, on the other hand, shows strong intermolecular H–F interactions as well as intramolecular S–F and S–N interactions that help to minimize conformational disorder; interactions that are likely to be factors greatly contributing to the stronger crystal lattice of DTF2BT.

## CONCLUSIONS

In summary, to unambiguously compare the important chromophores DTBT and DTF2BT, a task that is often obscured by other parameters such as molecular weight differences and solubility issues upon comparison of the corresponding polymers, their crystal structures were determined and thoroughly analyzed in this work. These data were supported by  $^1\text{H NMR}$ , UV–vis, and DSC data as well as quantum mechanical calculations. While DTBT packs with a slightly better cofacial overlap, DTF2BT shows more prominent intra- and intermolecular interactions, which can be particularly important for long-range charge transport in organic electronic materials.  $^1\text{H NMR}$  studies furthermore indicated that the flanking thiophene groups can rotate freely even at low temperatures, which is in agreement with the conformational disorder observed for both structures in the solid state. UV–vis spectroscopy showed that DTF2BT is slightly blue-shifted and has a molar absorptivity higher than that of DTBT, which is of obvious importance for photovoltaic applications. DTBT has a permanent dipole moment significantly larger than that of DTF2BT, which affects the solid state packing and is also thought to affect the distribution of conformational orientations in solutions of varying polarity.

## ASSOCIATED CONTENT

### Supporting Information

Additional information about the single-crystal structures, the variable-temperature  $^1\text{H NMR}$  studies, and the Gaussian-calculated energies of the molecular conformations of DTBT and DTF2BT. The Supporting Information is available free of charge on the ACS Publications website at DOI: 10.1021/acs.joc.5b00430.

## AUTHOR INFORMATION

### Corresponding Author

\*E-mail: c.nielsen@imperial.ac.uk.

## Notes

The authors declare no competing financial interest.

## ACKNOWLEDGMENTS

We are thankful for financial support from EC FP7 Project X10D, EC FP7 Project SC2, and EC FP7 Project PolyMed.

## REFERENCES

- (1) Tsao, H. N.; Cho, D. M.; Park, I.; Hansen, M. R.; Mavrinskiy, A.; Yoon, D. Y.; Graf, R.; Pisula, W.; Spiess, H. W.; Müllen, K. *J. Am. Chem. Soc.* **2011**, *133*, 2605.
- (2) Zhang, X.; Bronstein, H.; Kronemeijer, A. J.; Smith, J.; Kim, Y.; Kline, R. J.; Richter, L. J.; Anthopoulos, T. D.; Sirringhaus, H.; Song, K.; Heeney, M.; Zhang, W.; McCulloch, I.; DeLongchamp, D. M. *Nat. Commun.* **2013**, *4*, 2238.
- (3) Peet, J.; Kim, J. Y.; Coates, N. E.; Ma, W. L.; Moses, D.; Heeger, A. J.; Bazan, G. C. *Nat. Mater.* **2007**, *6*, 497.
- (4) Nielsen, C. B.; Schroeder, B. C.; Hadipour, A.; Rand, B. P.; Watkins, S. E.; McCulloch, I. *J. Mater. Chem.* **2011**, *21*, 17642.
- (5) Parker, T. C.; Patel, D. G.; Moudgil, K.; Barlow, S.; Risko, C.; Bredas, J.-L.; Reynolds, J. R.; Marder, S. R. *Mater. Horiz.* **2015**, *2*, 22.
- (6) Zhou, P.; Zhang, Z.-G.; Li, Y.; Chen, X.; Qin, J. *Chem. Mater.* **2014**, *26*, 3495.
- (7) Fan, L.; Cui, R.; Guo, X.; Qian, D.; Qiu, B.; Yuan, J.; Li, Y.; Huang, W.; Yang, J.; Liu, W.; Xu, X.; Li, L.; Zou, Y. *J. Mater. Chem. C* **2014**, *2*, 5651.
- (8) Nielsen, C. B.; Ashraf, R. S.; Treat, N. D.; Schroeder, B. C.; Donaghey, J. E.; White, A. J. P.; Stingelin, N.; McCulloch, I. *Adv. Mater.* **2015**, *27*, 948.
- (9) Zhou, H.; Yang, L.; Stuart, A. C.; Price, S. C.; Liu, S.; You, W. *Angew. Chem., Int. Ed.* **2011**, *50*, 2995.
- (10) Schroeder, B. C.; Ashraf, R. S.; Thomas, S.; White, A. J. P.; Biniak, L.; Nielsen, C. B.; Zhang, W.; Huang, Z.; Tuladhar, P. S.; Watkins, S. E.; Anthopoulos, T. D.; Durrant, J. R.; McCulloch, I. *Chem. Commun.* **2012**, *48*, 7699.
- (11) Bronstein, H.; Frost, J. M.; Hadipour, A.; Kim, Y.; Nielsen, C. B.; Ashraf, R. S.; Rand, B. P.; Watkins, S.; McCulloch, I. *Chem. Mater.* **2013**, *25*, 277.
- (12) Jackson, N. E.; Savoie, B. M.; Kohlstedt, K. L.; Olvera de la Cruz, M.; Schatz, G. C.; Chen, L. X.; Ratner, M. A. *J. Am. Chem. Soc.* **2013**, *135*, 10475.
- (13) Curtis, M. D.; Cao, J.; Kampf, J. W. *J. Am. Chem. Soc.* **2004**, *126*, 4318.
- (14) Kwon, O.; Coropceanu, V.; Gruhn, N. E.; Durivage, J. C.; Laquindanum, J. G.; Katz, H. E.; Cornil, J.; Brédas, J. L. *J. Chem. Phys.* **2004**, *120*, 8186.
- (15) Subramanian, S.; Park, S. K.; Parkin, S. R.; Podzorov, V.; Jackson, T. N.; Anthony, J. E. *J. Am. Chem. Soc.* **2008**, *130*, 2706.
- (16) Risko, C.; McGehee, M. D.; Bredas, J.-L. *Chem. Sci.* **2011**, *2*, 1200.
- (17) Sherrill, C. D.; Takatani, T.; Hohenstein, E. G. *J. Phys. Chem. A* **2009**, *113*, 10146.